

# Radiation Patterns of RF Aperture Antennas

Dan Lenski, Matt Siegler, and Adam Mantz

November 6, 2002

## Abstract

Radiation patterns of a Gunn oscillator emitting modulated RF radiation are measured with feed horn antennas. In one configuration, the radiation pattern is measured with a single antenna, while in another the radiation pattern is measured with a pair of antennas in an adding interferometer configuration. Measured radiation patterns are compared to theoretical predictions.

## 1 Introduction

Our setup consists of a fixed Gunn oscillator and a set of two small horn antennas about 5 m away ( $R \gg D^2/\lambda$ , far-field approximation holds). The Gunn oscillator is fed by a 12.0 V power source outputting square waves with a frequency of 1.00 kHz. The modulated oscillator emits microwave-band radiation at  $\lambda = 2.64$  cm.

The antennas are fixed at a baseline separation of  $B = 20.22$  cm, and each has horn dimensions of  $7.30 \times 5.45$  cm ( $a \times b$ ). Their aperture openings are parallel, and the entire setup may be rotated with polar and azimuthal motors. One antenna may be disabled so that a single-antenna radiation pattern can be studied.

The origins of the azimuthal and polar motors are necessarily arbitrary. The angles about these axes will be referred to as  $\hat{A}$  (azimuthal angle) and  $\hat{P}$  (polar angle) respectively, to differentiate them from  $\phi$  and  $\theta$ , which express the relative orientation of the antenna aperture and the Gunn oscillator. The boresight, the point of maximum received power, is at  $\hat{P} = 84^\circ$  and  $\hat{A} = 64^\circ$  in

our measurements. (Corresponding to the antennas pointed slightly downward from the horizontal, and across the room.)

The power received by the antenna setup is measured by a voltmeter (via a square-law detector). For the radiation patterns studied in the present report, the received power (voltage) was measured at  $2^\circ$  intervals over a range about the boresight, in each of the principal planes. For the interferometer horizontal-plane pattern, we went back and measured the angle and voltage at each of the fringe peaks, even if they lay in between on a  $2^\circ$  mark, in order to pinpoint them more accurately.

The  $(\hat{P}, \hat{A})$  motor axis angles are related to the  $(\theta, \phi)$  angles (discussed below) as follows:

$$\begin{aligned}\theta &= \sqrt{(\hat{P} - \hat{P}_0)^2 + (\hat{A} - \hat{A}_0)^2} \\ \phi &= \tan^{-1} \left( \frac{\hat{P} - \hat{P}_0}{\hat{A} - \hat{A}_0} \right)\end{aligned}$$

Thus, if  $\hat{P}$  is fixed at  $\hat{P}_0$ , this will correspond to the  $\phi = 0$  horizontal plane, while if  $\hat{A}$  is fixed at  $\hat{A}_0$ , this will correspond to the  $\phi = \pi/2$  elevation plane.

## 2 Methods

### 2.1 Theoretical Models of Antenna Radiation

Consider a rectangular aperture antenna centered at the origin in the  $x$ - $y$  plane, having dimension  $a$  in the  $x$ -direction and  $b$  in the  $y$ -direction (where  $a > b$ ), and emitting radiation in the  $+z$  direction. Now consider an observer at some distant point  $P$ . Let  $\theta$  be the angle between the  $+z$ -axis and a line joining  $P$  to the origin. Let  $(r \cos \phi, r \sin \phi)$  be the projection of point  $P$  onto the  $x$ - $y$  plane.

The relative electric field strength at point  $P$  compared to other points at the same distance is

$$\begin{aligned}E_{norm}(\phi, \theta) &= \frac{\sin(\pi \frac{b}{\lambda} \sin \theta \sin \phi)}{\pi \frac{b}{\lambda} \sin \theta \sin \phi} \times \cos(\pi \frac{a}{\lambda} \sin \theta \cos \phi) \\ &\times \left[ \frac{1}{2 - 4 \frac{a}{\lambda} \sin \theta \cos \phi} + \frac{1}{2 + 4 \frac{a}{\lambda} \sin \theta \cos \phi} \right].\end{aligned}$$

This far-field approximation was derived by Prof. Cordes in the handout and assumes zero phase error in the aperture. Because of the Reciprocity Principle, interchanging the observer and trans-

mitter will not affect the pattern. The power in the radiation is  $P = |E|^2$ , from basic E&M.

With two rectangular aperture antennas in an adding interferometer configuration, the received power can be related to the single-antenna power as follows:

$$\begin{aligned} E_{double}(\phi, \theta) &= 2E_{single}e^{-i\varphi/2} \cos \varphi \quad \text{where } \varphi = 2\pi \frac{B}{\lambda} \cos \phi \sin \theta \\ P_{double}(\phi, \theta) &= 4P_{single} \cos^2 \left( \pi \frac{B}{\lambda} \cos \phi \sin \theta \right) \end{aligned}$$

## 2.2 Determining FWHM

I estimated the full-width half-maximum beamwidth for the single horn radiation patterns by measuring the maximum intensity values for each principal plane, then using linear interpolation of the measured data to find the two angles at which the half-maximum value was achieved, one on either side of the boresight. I then took the difference between these two angles to find the beamwidth.

**Example:** Computing the FWHM in the horizontal plane (polar axis motor fixed). The maximum value of 0.181 V occurs at  $64^\circ$ . Thus we want to find the angles at which  $V = 0.0950$  V in order to compute the FWHM.

The closest measured data points are:  $V = 0.106$  V at  $\hat{A} = 74^\circ$ ,  $V = 0.071$  V at  $\hat{A} = 76^\circ$ ; and  $V = 0.103$  V at  $\hat{A} = 50^\circ$ ,  $V = 0.086$  V at  $\hat{A} = 48^\circ$ . Linear interpolation from the first pair gives  $V = 0.0905$  V at  $\hat{A} \approx 74.9^\circ$ , and from the second pair,  $V = 0.0905$  V at  $\hat{A} \approx 48.5^\circ$ . Thus the FWHM is  $|74.9^\circ - 48.53^\circ| = 26.4^\circ$ .

## 2.3 Computer Programs

I wrote two computer programs in Perl to aid in the data reduction and analysis for this report. They both manipulate data in the simple text file format used by `gnuplot`, which was used to produce all the graphics. This file format consists of fields for each data point ( $x$  and  $y$  values) separated by spaces, each data point on a separate line.

## Theoretical Radiation Patterns: radpats.pl

This program computes the theoretical zero phase-error radiation patterns for: (a) a single antenna in the  $\phi = 0$  plane (H-plane); (b) a single antenna in the  $\phi = \pi/2$  plane (E-plane); (c) a two-antenna interferometer in the  $\phi = 0$  plane; and (d) a two-antenna interferometer in the  $\phi = \pi/2$  plane. (Extra credit for the interferometer patterns.)

The program outputs a gnuplot data file for each pattern, containing both linear and logarithmic values for the power distribution at  $0.25^\circ$  intervals. The output is aligned in overall amplitude and angular offset with the corresponding plot of measured data from our experiments, so that the two may be graphed together for comparison.

```
#!/usr/bin/perl
use Math::Trig;
sub decibels { 10 * log($_[0]) / log(10) }

#####
# Parameters of our setup
#####

$a = 7.3; #cm - larger horn dimension
$b = 5.45; #cm - smaller horn dimension
$lam = 2.64; # cm - wavelength
$nu = 29979245800 / $lam; # Hz - frequency
$B = 20.22; #cm - baseline
$D = 500; #cm - transmitter/receiver distance

#####
# Single horn field formula
#####

sub sinxoverx { $_[0] ? (sin($_[0])/$_[0]) : 1 }
sub Enorm($$)
{
    my ($th, $phi) = @_;

    $factor1 = sinxoverx(pi*($b/$lam)*sin($th)*sin($phi));
    $factor2 = cos(pi*($a/$lam)*sin($th)*cos($phi));
    $factor3 = 1/(2 - 4*($a/$lam)*sin($th)*cos($phi))
              + 1/(2 + 4*($a/$lam)*sin($th)*cos($phi));
    return ($factor1 * $factor2 * $factor3);
}

#####
```

```

# Single Horn (Varying Polar Angle) plane pattern
#####

open OUT, ">sh_pol_theory.gnuplot";
print OUT <<EOF;
#Single Horn, varying polar angle (phi fixed at max)
#Theoretical power pattern
#
#Phi (deg) V (volts) P (dB) ||| Phi (max at 0) P (unscaled)
EOF

$amp = 0.186; # amplitude scale factor
$thdeg0 = 84; # degrees - angle offset
for ($thdeg=-90; $thdeg <= 90; $thdeg+=0.25) {
    $th = deg2rad($thdeg);
    $phi = pi/2;

    $E = Enorm($th, $phi) / Enorm(0, $phi); # Field (normalized to 1 at boresight)
    $P = $E**2; # Power
    $X = decibels($P); # Power (log scale)

    printf OUT ("%g %g %g ||| %g %g\n",
                $thdeg+$thdeg0, $P*$amp, $X, $thdeg, $P);
}
close OUT;

#####
# Single Horn (Varying Azimuthal Angle) plane pattern
#####

open OUT, ">sh_az_theory.gnuplot";
print OUT <<EOF;
#Single Horn, varying azimuthal angle (theta fixed at max)
#Theoretical power pattern
#
#Phi (deg) V (volts) P (dB) ||| Phi (max at 0) P (unscaled)
EOF

$amp = 0.181; # amplitude scale factor
$thdeg0 = 64; # degrees - angle offset
for ($thdeg=-90; $thdeg <= 90; $thdeg+=0.25) {
    $th = deg2rad($thdeg);
    $phi = 0;

    $E = Enorm($th, $phi) / Enorm(0, $phi); # Field (normalized to 1 at boresight)
    $P = $E**2; # Power
    $X = decibels($P); # Power (log scale)
}

```

```

        printf OUT ("%g %g %g ||| %g %g\n",
                    $thdeg+$thdeg0, $P*$amp, $X, $thdeg, $P);
    }
close OUT;

#####
# Double Horn (Varying Polar Angle) plane pattern
#####

open OUT, ">dh_pol_theory.gnuplot";
print OUT <<EOF;
#Double Horn, varying polar angle (phi fixed at max)
#Theoretical power pattern
#
#Theta (deg) V (volts) I (dB)
EOF

$amp = 0.690; # amplitude scale factor
$thdeg0 = 84; # degrees - angle offset
for ($thdeg=-90; $thdeg <= 90; $thdeg+=0.25) {
    $th = deg2rad($thdeg);
    $phi = pi/2;

    $E = Enorm($th, $phi) * cos(pi*($B/$lam)*cos($phi)*sin($th))
        / Enorm(0, $phi);          # Field (normalized to 1 at boresight)
    $P = $E**2;                    # Power
    $X = decibels($P);              # Power (log scale)

    printf OUT ("%g %g %g ||| %g %g\n",
                $thdeg+$thdeg0, $P*$amp, $X, $thdeg, $P);
}
close OUT;

#####
# Double Horn (Varying Azimuthal Angle) plane pattern
#####

open OUT, ">dh_az_theory.gnuplot";
print OUT <<EOF;
#Double Horn, varying azimuthal angle (theta fixed at max)
#Theoretical power pattern
#
#Phi (deg) V (volts) P (dB) ||| Phi (max at 0) P (unscaled)
EOF

$amp = 0.748; # amplitude scale factor

```

```



```

### Peak Finder: find\_peaks.pl

This program takes a gnuplot data file as an argument. It expects the fields for each data point to be an angle and a voltage, and it prints out the angles at which the voltage is at a local maximum, relative to the boresight angle (overall maximum voltage).

```

#!/usr/bin/perl

# Read "<angle> <voltage>" from input file.
while (<>) {
    next if /^#\;/; # skip comments
    chomp;
    (

```

### 3 Results and Discussion

#### 3.1 Single Horn Antenna

I found that, in the horizontal plane ( $\phi = 0$ ), the FWHM of the measured radiation pattern was  $26.4^\circ$ . In the vertical plane ( $\phi = \pi/2$ ), the FWHM was  $23.1^\circ$ .

This agrees fairly well with theory: in the horizontal plane, the radiation pattern is predicted to be

$$E_{norm}(\theta, 0) = \cos\left(\pi\frac{a}{\lambda}\sin\theta\right) \cdot \left[ \frac{1}{2 - 4\frac{a}{\lambda}\sin\theta} + \frac{1}{2 + 4\frac{a}{\lambda}\sin\theta} \right].$$

The maximum value will be at  $\theta = 0$ . We want to find angles for which  $E_{norm}(\theta, \phi) = 1/2$  (the half max points). This value is found numerically to occur around  $\pm 12.4^\circ$ , giving a FWHM of  $24.8^\circ$ . Thus our measured value is 6.5% higher than this theoretical predicted value.

In the vertical plane, the radiation pattern is predicted to be

$$E_{norm}(\theta, \pi/2) = \frac{\sin\left(\pi\frac{b}{\lambda}\sin\theta\right)}{\pi\frac{b}{\lambda}\sin\theta}.$$

This is maximized at  $\theta = 0$ , and half-maximum values occur around  $\pm 12.4^\circ$  again, giving a FWHM of  $24.8^\circ$  again. Our measured value for the FWHM in this plane is 6.85% below the prediction.

Of course, these two theoretical values for the FWHM assume that the aperture antenna has zero phase error. Taking phase error into account, Prof. Cordes calculated the FWHM for the vertical plane to be  $27.8^\circ$  in the horizontal plane, and  $25.6^\circ$  in the vertical plane. These agree more closely with our measured values. Using these phase-error-corrected FWHM predicted values, our measurements are off by 5.03% for the horizontal plane and 3.12% for the vertical plane.

The two radiation patterns are not identical. However, the differences seem to be due to measurement errors and problems with the geometry of the room. The theory predicts that the two patterns should be extremely similar to within about  $20^\circ$  of the boresight; the vertical plane pattern will then drop off to a null a few degrees before the horizontal plane pattern. This is apparently true from our measured patterns: the nulls of the vertical pattern occur slightly closer to the boresight than those of the horizontal plane pattern. It is difficult to decide if this result is significant, or simply a lucky coincidence, due to the roughness of our measurements.

Theory predicts that both radiation patterns should be perfectly symmetrical. Ours, however, are not. Particularly odd is the large “bump” in the horizontal plane radiation pattern at around

50°. This and other irregularities are perhaps attributable to the sensitivity of the experiment to the geometry of the room in which it was performed. Moving a backpack on a table or standing too close to the beam could easily affect the measured power by several percent.

Another anomaly is that the top of our measured pattern for the vertical plane is much narrower (drops off much more rapidly around the boresight) than the theoretically predicted pattern. We repeated these measurements several times, but found this effect each time.

The theory predicts that the sidelobes on the vertical plane pattern should be much larger than those on the horizontal plane pattern. It was not possible to measure the sidelobes in the horizontal plane pattern because the power dropped below the sensitivity of the voltmeter used to measure it. In the vertical plane, we stopped measuring the power at the points when the beam was pointing at solid objects, namely the table and the metal bars in the ceiling.

It does appear from our horizontal-plane measured pattern that the sidelobes are higher and blurrier than would be expected for zero phase error. At the points where we stopped measuring they were higher than the expected nulls. This is consistent with the picture of blurry raised sidelobes and nulls given by the phase-error-corrected plots in Figure (10) of the packet.

### 3.2 Double-Horn Interferometer

Theory predicts that the power received from (or transmitted by) a pair of feed horns will be  $4 \cos^2(\pi \frac{B}{\lambda} \cos \phi \sin \theta)$  times that of a single horn at the same orientation. Thus, if we hold  $\phi$  fixed at  $\pi/2$ , the power will be simply four times that of a single horn. This corresponds to the radiation pattern in the vertical plane.

In the vertical plane, our measurements conformed closely to this theoretically predicted curve, and the boresight voltage 0.690 V, was 3.71 times that of the single horn. The measurements deviated from the model much less than in the single-horn measurements for the vertical plane, perhaps because the two horns tended to “damp each other out,” so that a local inaccuracy in one horn (i.e. due to the geometry of the room) would be a smaller proportion of the total power.

In the horizontal ( $\phi = 0$ ) plane, on the other hand, the power of a double-horn interferometer will be  $4 \cos^2(\pi \frac{B}{\lambda} \sin \theta)$  times that of a single horn. For our values of  $B = 20.22$  cm and  $\lambda = 2.64$  cm, this comes out to  $E_{double} = 4 \cos^2(7.659\pi \sin \theta) E_{single}$ , and thus we predict a pattern of fringes, with

peaks at all values of  $\theta$  such that  $\cos(7.659\pi \sin \theta) = \pm 1$  ( $n$  an integer), and thus  $\sin \theta = n/7.659$ .

Therefore peaks are predicted to occur at  $\theta = 0^\circ, \pm 7.5^\circ, \pm 15.1^\circ, \pm 23.0^\circ, \pm 31.4^\circ, \pm 40.7^\circ, \pm 51.5^\circ, \text{ and } \pm 66.0^\circ$ . These angles are relative to the boresight, as usual. Beyond  $66.0^\circ$  no peaks will occur, because for  $n > 7$ , the above equation yields complex solutions for  $\theta$ !

<b>Predicted Peak</b>	<b>Measured Peaks</b>		<b><math> \langle \text{Measured} \rangle  -  \text{Predicted} </math></b>
$0^\circ$	$0^\circ$		$0^\circ$
$7.5^\circ$	$+8.0^\circ$	$-8.0^\circ$	$+0.50^\circ$
$15.1^\circ$	$+16.0^\circ$	$-16.0^\circ$	$+0.90^\circ$
$23.0^\circ$	$+23.0^\circ$	$-23.5^\circ$	$+0.25^\circ$
$31.4^\circ$	$+32.0^\circ$	$-29.5^\circ$	$-0.65^\circ$

As can be seen from the attached figure, the fringes in our measured radiation pattern tend to occur slightly further from the boresight than would be predicted by interferometer theory. This effect can probably be explained by the fact that these theoretical predictions fail to account for the phase error introduced in a finite-length feed horn.

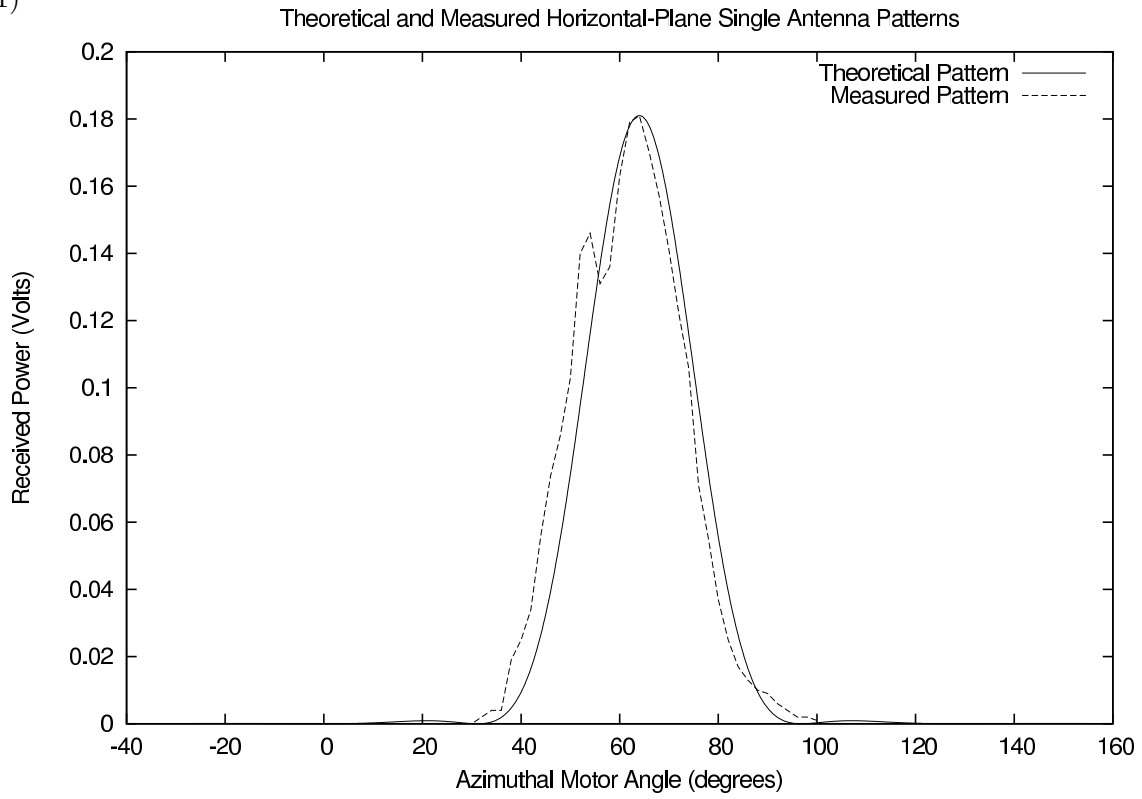
Also, the first two peaks to the left of the central bright fringe are of greater amplitude than is theoretically predicted, while those to the right are of lesser amplitude. This discrepancy is probably due to the geometry of the room: for angles  $< 84^\circ$ , the beam was pointed roughly towards a metal shelving unit, which might reflect some of the radiation.

## 4 Graphs

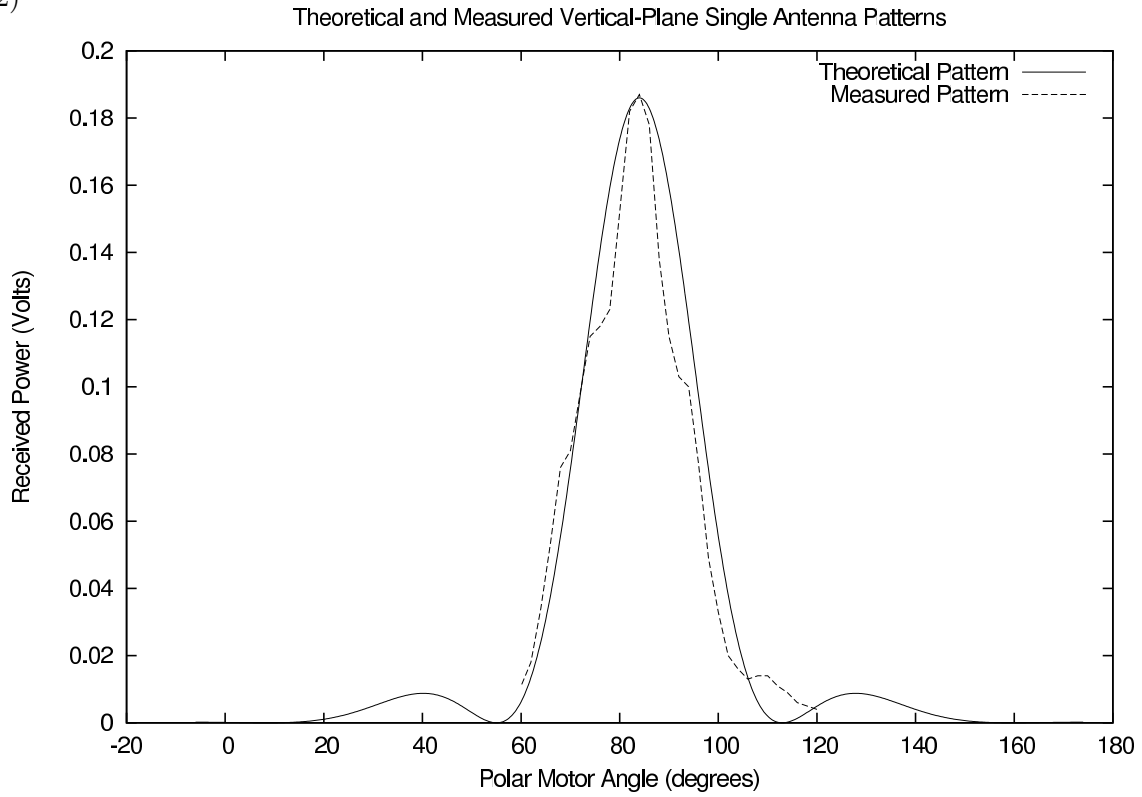
All theoretical patterns were calculated with the simplified theory of my `radpats.pl` program, which ignores phase error.

- 1— Theoretical and measured single horn radiation patterns (horizontal plane)
- 2— Single horn radiation patterns (vertical plane)
- 3— Interferometer radiation patterns, with predicted peaks (horizontal plane)
- 4— Interferometer radiation pattern (vertical plane)
- 5— Logarithmic power plot of theoretical single horn radiation patterns (both planes)

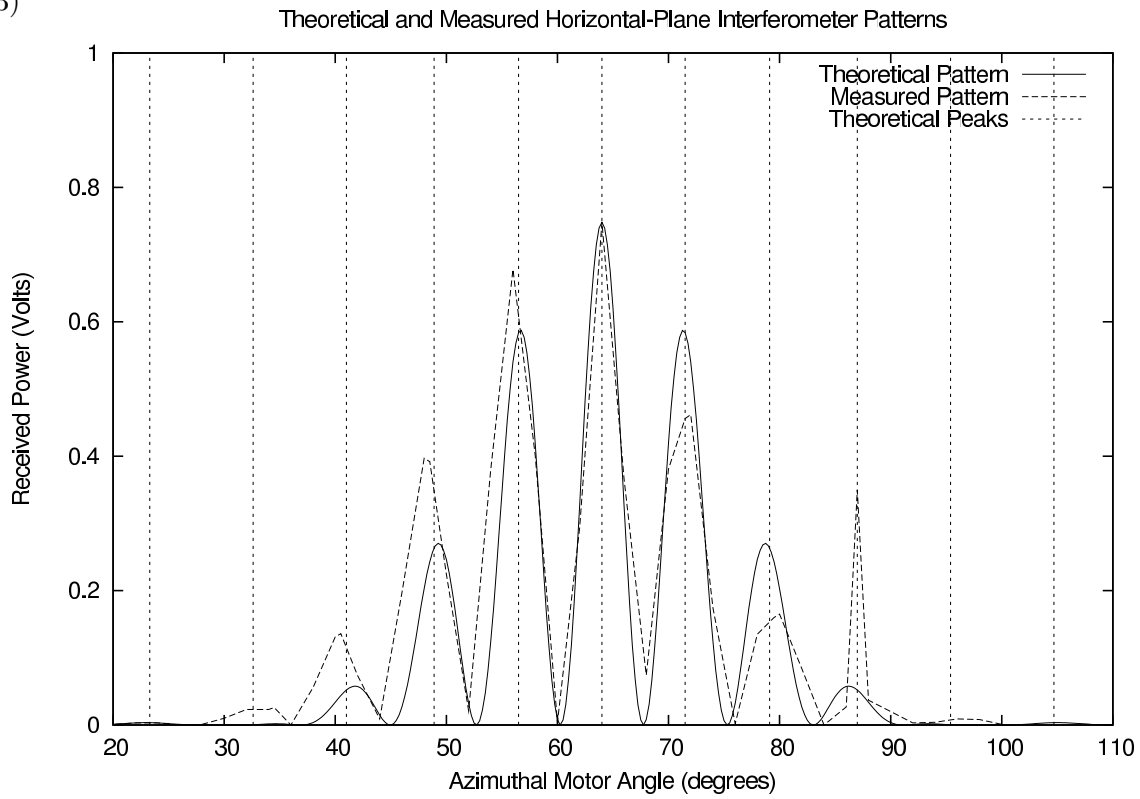
(1)



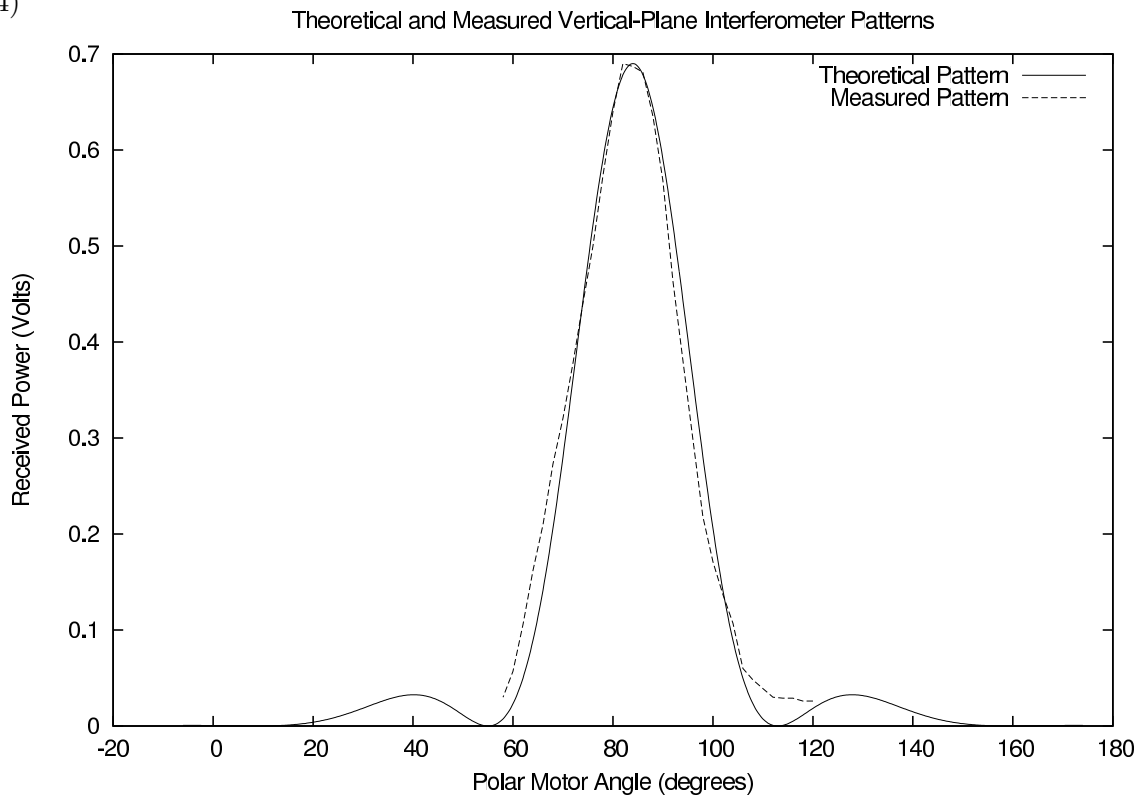
(2)



(3)



(4)



(5)

